New Expi293 suite of products for structural biology, inducible expression, and protein labeling

Learn more

THE PROTEIN SOCIETY

Not as easy as π: An insertional residue does not explain the π-helix gain-of-function in two-component FMN reductases

Jeffrey S. McFarlane,[2] Richard A. Hagen,[1] Annemarie S. Chilton,[2] Dianna L. Forbes,[1] Audrey L. Lamb,[2] and Holly R. Ellis [1]*

[1]The Department of Chemistry and Biochemistry, Auburn University, Auburn, Alabama, 36849
[2]The Department of Molecular Biosciences, University of Kansas, Lawrence, Kansas, 66045

Received 10 July 2018; Accepted 27 August 2018
DOI: 10.1002/pro.3504
Published online 15 November 2018 proteinscience.org

Abstract: The π-helix located at the tetramer interface of two-component FMN-dependent reductases contributes to the structural divergence from canonical FMN-bound reductases within the NADPH: FMN reductase family. The π-helix in the SsuE FMN-dependent reductase of the alkanesulfonate monooxygenase system has been proposed to be generated by the insertion of a Tyr residue in the conserved α4-helix. Variants of Tyr118 were generated, and their X-ray crystal structures determined, to evaluate how these alterations affect the structural integrity of the π-helix. The structure of the Y118A SsuE π-helix was converted to an α-helix, similar to the FMN-bound members of the NADPH: FMN reductase family. Although the π-helix was altered, the FMN binding region remained unchanged. Conversely, deletion of Tyr118 disrupted the secondary structural properties of the π-helix, generating a random coil region in the middle of helix 4. Both the Y118A and Δ118 SsuE SsuE variants crystallize as a dimer. The MsuE FMN reductase involved in the desulfonation of methanesulfonates is structurally similar to SsuE, but the π-helix contains a His insertional residue. Exchanging the π-helix insertional residue of each enzyme did not result in equivalent kinetic properties. Structure-based sequence analysis further demonstrated the presence of a similar Tyr residue in an FMN-bound reductase in the NADPH:FMN reductase family that is not sufficient to generate a π-helix. Results from the

Abbreviations: FMN, oxidized flavin mononucleotide; $FMNH_2$, reduced flavin mononucleotide; NADPH, reduced nicotinamide adenine dinucleotide phosphate; NADH, reduced nicotinamide adenine dinucleotide; SsuE, alkanesulfonate monooxygenase flavin reductase; SsuD, alkanesulfonate monooxygenase; SfnF, dimethylsulfone monooxygenase flavin reductase; SfnG, dimethylsulfone monooxygenase; MsuE, methanesulfonate monooxygenase flavin reductase; MsuD, methanesulfonate monooxygenase.

Additional Supporting Information may be found in the online version of this article.

Impact statement: Two-component flavin-dependent enzymes consist of a flavin reductase and a flavin-dependent monooxygenase that utilize a comprehensive range of structural features to carry out their innovative mechanistic strategies. We have performed kinetic and structural studies to evaluate the relationship between distinct structural properties of the two-component FMN-dependent reductases with their overall function. The results obtained from these studies can be broadly applied to other enzymes that utilize similar structural features to enhance catalytic function.

Grant sponsor: NIGMS Graduate Training Program in the Dynamic Aspects of Chemical Biology (T32 GM008545); Grant sponsor: National Science Foundation Division of Chemistry (CHE-1403293); Grant sponsor: National Science Foundation Division of Molecular and Cellular Biosciences (MCB-1244320); Grant sponsor: Department of Energy Office of Biological and Environmental Research; Grant sponsor: U.S. Department of Energy, Office of Science, Office of Basic Energy Sciences; Grant sponsor: American Heart Association Predoctoral Fellowship (18PRE33960374).

*Correspondence to: Holly R. Ellis, Department of Chemistry and Biochemistry, Auburn University, Auburn, AL 36849.
E-mail: ellishr@auburn.edu

structural and functional studies of the FMN-dependent reductases suggest that the insertional residue alone is not solely responsible for generating the π-helix, and additional structural adaptions occur to provide the altered gain of function.

Keywords: flavin reductases; flavin monooxygenases; two-component FMN-dependent systems; π-helix; NAD(P)H-FMN reductase family; SsuE; SsuD; MsuE; MsuD

Introduction

In the majority of flavoprotein monooxygenases, the flavin is tightly bound and both the reductive and oxidative half-reactions occur on the same enzyme. However, a group of flavoprotein monooxygenases have been identified that rely on a separate flavin-dependent reductase to catalyze the reductive half reaction, with the reduced flavin transferred to a flavin-dependent monooxygenase to catalyze the oxidative half reaction generating an oxygenated product. While the substrates for the monooxygenases of two-component systems are quite diverse, several FMN-dependent two-component monooxygenase systems have been identified that are involved in bacterial sulfur acquisition. A common means for acquiring sulfur during sulfur limitation in diverse bacteria is the two-component alkanesulfonate monooxygenase system [Fig. 1(A)]. The majority of kinetic studies have focused on the alkanesulfonate monooxygenase system in *Escherichia coli*.[1–6] but these systems are widely conserved suggesting an essential role in maintaining cellular sulfur concentrations.[7] *Pseudomonas* sp. have a more complex mechanism for sulfur acquisition when sulfur in the environment is limiting.[8] Certain pseudomonads contain multiple two-component FMN-dependent systems that form a pathway to convert dimethylsulfone ($DMSO_2$) to sulfite, but also allow them to utilize long-chain aliphatic sulfonates. $DMSO_2$ is derived through the oxidation of dimethyl sulfide, a secondary metabolite in some marine algae, and is the most abundant biological sulfur compound emitted to the atmosphere.[9] $DMSO_2$ is converted to methanesulfinate by dimethylsulfone monooxygenase (SfnF/SfnG) [Fig. 1(B)].[10–14] The methanesulfinate produced is oxidized in some *Pseudomonas* sp. to methanesulfonate by the methanesulfinate monooxygenase system (MsuE/MsuC) [Fig. 1(C)], and the methanesulfinate is further oxidized to sulfate and formaldehyde by methanesulfonate monooxygenase (MsuE/MsuD) [Fig. 1(D)].[15] *Pseudomonas aeruginosa* contains a complete pathway for the conversion of $DMSO_2$ to sulfite release.

Two NAPDH:FMN reductases with high structural similarity to SsuE are YdhA from *Bacillus subtilis* and ArsH from *Shigella flexneri*.[16–18] The YdhA enzyme is classified as a quinone reductase, and ArsH is a reductase involved in arsenic resistance.[17–20] Unlike the reductases of the two-component systems, YdhA and ArsH do not require a monooxygenase partner, performing the oxidation of substrate molecules themselves. All four enzymes—YdhA, ArsH, SfnF, and SsuE—are grouped into the NAD(P)H:FMN reductase family based on the flavodoxin fold. These enzymes are further divided into subgroups of the family based on helix 4. While helix 4 in YdhA and ArsH is an α-helix, in the two-component FMN-dependent reductases, helix 4 is a π-helix structure. The π-helix is characterized by a wider turn due to $i + 5 \rightarrow i$ hydrogen bonding that causes a bulge in the helix. It has been proposed that π-helices arise due to an amino acid insertion in an established α-helix, which becomes the basis of a new structural element with a defined function. The π-helix has been proposed to provide a gain-of-function, thereby counterbalancing the relative structural instability compared to a continuous α-helix. Specified functional roles

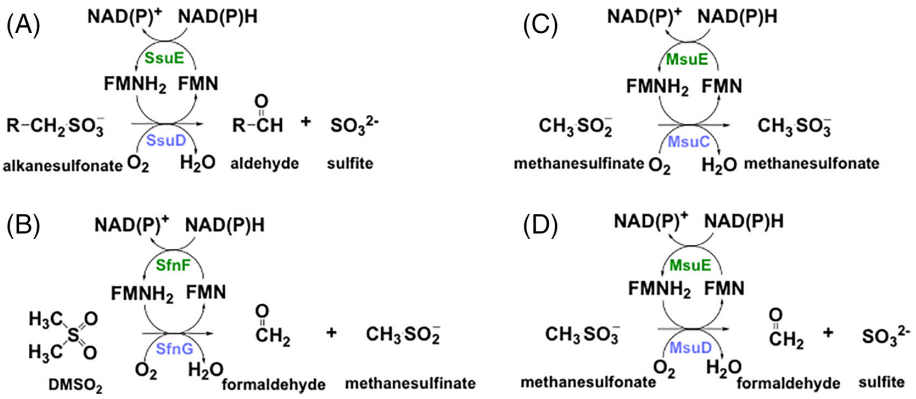

Figure 1. Reactions of two-component systems involved in sulfur metabolism. Two-component FMN-dependent monooxygenase reactions found in different bacterial organisms: (A) alkanesulfonate monooxygenase reaction (SsuE/SsuD); (B) dimethysulfone monooxygenase reaction (SfnF/SfnG), (C) methanesulfinate monooxgenase reaction (MsuE/MsuC); (D) methanesulfonate monooxygenase reaction (MsuE/MsuD).

for π-helices have been experimentally identified in a limited number of proteins, and include active site features to promote metal or cofactor binding, or introduction of catalytic residues.[21,22]

The π-helix in SsuE has been proposed to be generated by the insertion of a Tyr residue in the conserved α4-helix.[16] In the three-dimensional structure of apo-SsuE (PDB 4PTY), π-stacking interactions are observed between the aromatic rings of Tyr118 residues across the tetramerization interface. In a flavin-bound SsuE structure, the hydroxyl group of Tyr118 hydrogen bonds to the oxygen atom backbone carbonyl of Ala78 across the tetramer interface; however, this structure was generated by soaking tetrameric crystals with excess flavin.[16] In solution, the SsuE enzyme has been shown to undergo a tetramer to dimer oligomeric change upon binding of FMN [Fig. 2(A)], and this oligomeric change may promote protein–protein interactions that facilitate the release of reduced flavin to SsuD [Fig. 2(B,C)]. Therefore, the π-helix may provide a gain-of-function by promoting the release of reduced flavin to the monooxygenase. Previous studies showed that conversion of Tyr118 to alanine (Y118A SsuE) generated protein that stably bound oxidized FMN and showed no NADPH oxidase activity.[23,24] A deletion variant of Tyr118 (ΔY118 SsuE) was not purified with FMN bound, but the variant also lacked reductase activity. While the initial flavin reduction was observed in the SsuE variants, the $FMNH_2$ was trapped in the closed active site preventing steady-state reductase activity.[23] Although the FMN was reduced, both Y118A and ΔY118 SsuE were also unable to support desulfonation by the SsuD monooxygenase.

In addition to modification of the kinetic properties, variants of Tyr118 showed altered oligomeric states compared to wild-type SsuE.[23,24] Whereas apo wild-type enzyme is tetrameric in solution and in crystals, addition of FMN promotes conversion to a dimeric state.[25] In the structure of wild-type SsuE, the Tyr118 insertional residue sits near the 222 symmetry of the tetramer, but it is not known how FMN binding alters contacts to promote the conversion from tetramer to dimer. The structure of FMN-bound wild-type SsuE was determined by soaking apo crystals in a large excess of FMN. Therefore, the oligomerization state is the result of the crystal lattice of the apo-protein and does not represent the physiological oligomeric state upon FMN binding. The Y118A variant is dimeric in solution.[23] Taken together, the above data suggest that removing the tyrosine sidechain (Y118A) prevents flavin release and also suggest that the transition from the tetrameric to dimeric state may be important in FMNH2 transfer from SsuE to the monooxygenase SsuD. Deletion of Tyr118 (ΔY118 SsuE) also eliminates reductase activity; however, this variant was tetrameric in solution.[23] We hypothesized that in both Y118A and ΔY118 SsuE, helix 4 would be a continuous α-helix due to removal of the tyrosine insertional residue.

In *Pseudomonas putida* SfnF (PDB 4C76—we note that this protein is misannotated in the PDB as MsuE), the insertional residue is a histidine (His128), which potentially plays a similar π-stacking role as Tyr118 SsuE. Amino acid sequence analyses and structural modeling of MsuE from *P. aeruginosa* indicate that the overall structure is similar to SsuE and SfnF, with a π-helix His insertional residue. Therefore, we tested the hypothesis that interchanging the π-helix insertional residues would generate variant proteins, Y118H and H126Y MsuE, with kinetic properties consistent with those of the wild-type enzyme.

Results

Preparation of Y118A and ΔY118 SsuE

Crystal structures of π-helix variants Y118A SsuE, with and without FMN, and ΔY118 SsuE without FMN were obtained to high resolution (all better than 2 Å) to assess how variations at the critical

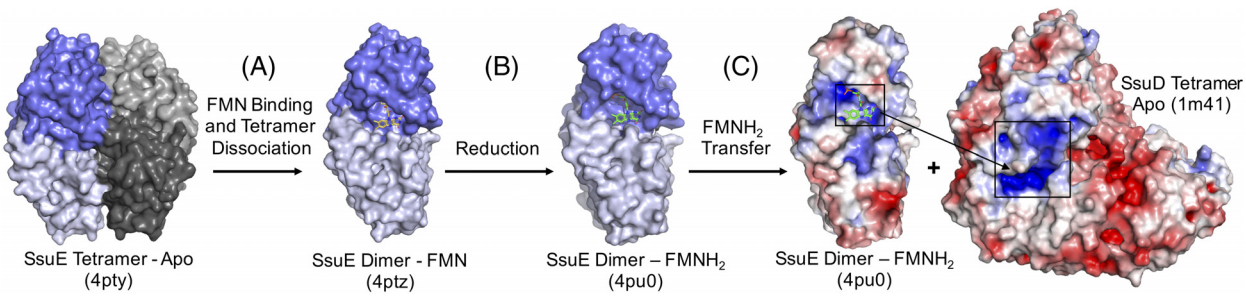

Figure 2. Structural scheme for the mechanism of the two-component alkanesulfonate monooxygenase system. (A) The tetramer of SsuE (monomers for dimers are shades of gray and blue) binds FMN (yellow carbons), and dissociates to a dimer. (B) FMN is reduced by NAD(P)H to $FMNH_2$ (green carbons). (C) Electrostatic surface views of SsuE and SsuD (blue, positive charge; red, negative charge). $FMNH_2$-bound SsuE associates with SsuD and transfers the reduced flavin to the SsuD monooxygenase. The predicted SsuD active site region is boxed, and has a charged surface complementary to the $FMNH_2$ binding region of the SsuE dimer. The apo, FMN-bound, and $FMNH_2$ SsuE structures were rendered with PDB: 4PTY, 4PTZ, and 4PU0, respectively. The SsuD structure was rendered with PDB 1M41.[16]

π-helix alter the structure and potentially contribute to changes in function. The previously published crystallization conditions for wild-type did not produce diffraction quality crystals for Y118A SsuE and produced no crystals for ΔY118 SsuE; thus, it became necessary to screen for new conditions. Indeed, each variant structure determined in these studies was from an independent crystallization condition. The original conditions for wild-type protein used PEG3350 as a precipitant and citrate as an additive. The apo Y118A SsuE structure was determined from crystals that used lithium sulfate as a precipitant. The FMN-bound Y118A SsuE crystals did use PEG3350 as a precipitant, but at more than double to concentration (20% as opposed to 7%), with thiocyanate as an additive. Finally, ΔY118 SsuE crystals required 30% PEG3000 as a precipitant. Not surprisingly, these different crystals were not isomorphous (different unit cell parameters and space groups) to each other or to the wild-type conditions.

Overall structure of π-helix variants

As with all structures determined to date, only the first 172–174 residues of 191 total are resolved in the maps. As expected, the monomers of the Tyr118 variants maintain a high overall structural conservation compared to the previously determined wild-type SsuE structure (PDB:4PTY), with root mean squared deviation values from 0.59 to 0.76 for 168–172 residues.[22] Unlike wild-type SsuE, which crystallizes as a tetramer, the Tyr118 variant structures determined here all crystallized as dimers [Fig. 3(A)]. The π-helices do not contribute to the dimeric assembly [Fig. 3(B)], and the variants show no difference at the dimeric interface compared to wild-type. The primary difference is found at the π-helix [Fig. 4(A)]. The Y118A SsuE variant no longer contained a π-helix, but instead helix 4 was a standard α-helix similar to that observed in ArsH and YdhA [Fig. 4(B)]. The original hypothesis was that the ΔY118 SsuE variant would also form a continuous α-helix for residues 110–127 through removal of the insertional tyrosine residue. However, the electron density maps clearly demonstrate that the deletion of residue 118 prevents a helical hydrogen bonding pattern for residues 115–119 (Supporting Information Fig.S2), causing the helix to be broken into two smaller helices N- and C-terminal to the deletion with a random coil for the intervening 4 residues [Fig. 4(B)].

FMN binding to Y118A SsuE

A superposition of Y118A SsuE with and without FMN bound demonstrates the same global fold, for the active site, with minor variances seen within the loop regions. The rmsd between apo and FMN-bound Y118A SsuE, 0.53–1.0 Å for 173 Cα, indicate their remarkable similarity, despite their differing crystallization conditions and unit cell parameters. Complete density for the active site FMN is present (Supporting Information Fig. S3). A second FMN that likely represents a crystallographic artifact is stacked along the isoalloxazine ring of the active site FMN with partial electron density for two conformations. A similar crystallographic FMN is observed in the FMN-bound wild-type structure.[16] In the wild-type structure, a hydrogen bond forms between the Tyr118 and a carbonyl oxygen of Ala78 from the opposing dimer, which in turn hydrogen bonds to the isoalloxazine ring system of the FMN. This network was hypothesized to aid in communication between the oligomerization interface and FMN binding.[16] While the Y118A SsuE variant clearly cannot hydrogen bond to Ala78 through the deleted hydroxyl, the Ala78–FMN hydrogen bond remains intact and the loop containing Ala78 has not shifted in

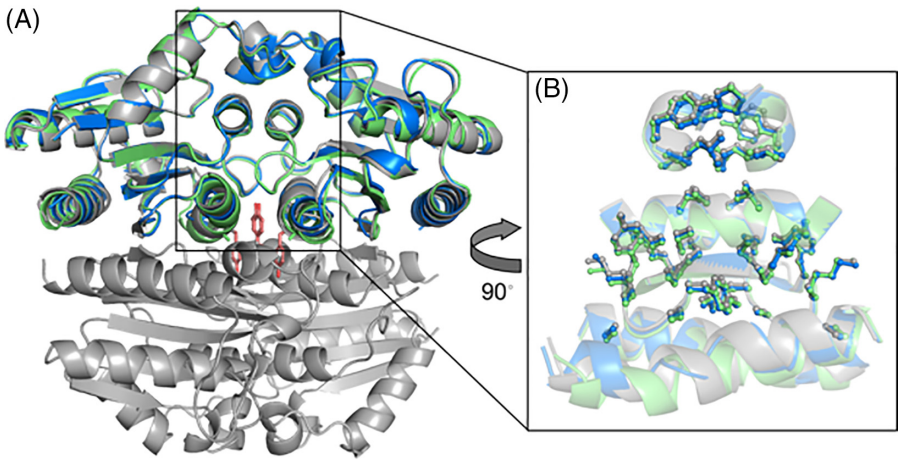

Figure 3. Oligomeric structures of the wild-type and Y118 SsuE variants. (A) Overlay of wild-type SsuE tetramer (gray with residue Y118 in orange) with dimers of apo Y118A SsuE (green) and Δ118 SsuE (blue) SsuE. The Y118A and Δ118 SsuE enzymes form the same homodimer as seen in the wild-type structure, but not the tetramer. (B) The position of the residues forming the 1160 Å^2 dimer interface remains the same in wild-type, Y118A, and Δ118 SsuE. The sidechains of the residues that make up the dimer interface are shown as ball-and-stick to emphasize their positional homology.

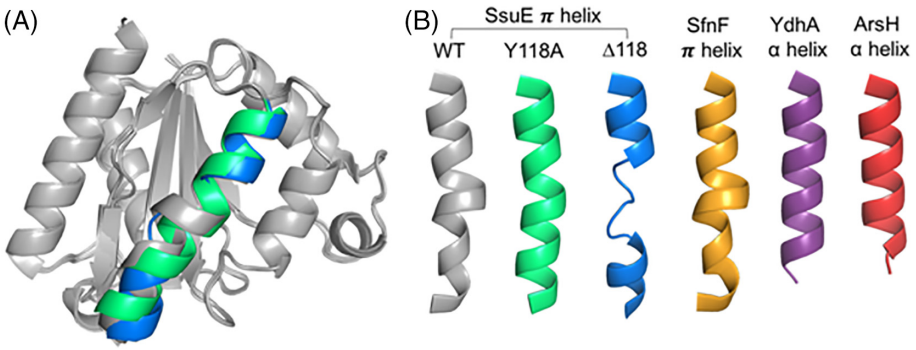

Figure 4. Comparison of π- and α-helical structures in the NADPH:FMN reductase family. (A) Overlay of the apo structures of wild-type (helix 4 gray), Y118A (helix 4 green) and ΔY118 (helix 4 blue) SsuE. (B) The π-helix in SsuE spans residues 110–127. The Y118A substitution results in the formation of a canonical α-helix, while the Y118 deletion prevents hydrogen bond formation between the carbonyls and amines of the amino acid backbone for residues 115–119 breaking the helical structure. The homolog SfnF (orange) with an inserted histidine forms a π-helix. In YdhA (purple) and ArsH (red), the tyrosine is absent and an α-helix is formed. SsuE (PDB:4PTY), Y118A SsuE (PDB:6DQI), ΔY118 SsuE (PDB:6DQP), SfnF (PDB:4C76), YdhA (PDB:2GSW), and ArsH (PDB:2Q62).[16–18]

conformation. The structure of the loop containing Ala78 is also maintained in the Δ118 SsuE structure.

Oligomeric assembly of π-helix variants

Comparison of the wild-type tetramer with the dimeric structures of FMN-bound Y118A and ΔY118 SsuE illustrates that key interactions composing the tetrameric interface are no longer possible (Fig. 5). The irregular helical turns in the wild-type π-helix provides a pattern of alternating hydrophobic residues that pack with the opposite homodimer (residues 110–114) [Fig. 5(A)]. The Y118A substitution results in helical turns of equal diameter (a continuous α-helix), but disrupts the hydrophobic packing pattern. This shift brings the N-termini of the helices in too close proximity for a stable interaction. Residues 111–114 take up new positions in the Y118A SsuE variant and reside in the three-dimensional space of the tetramerization interface of wild-type SsuE. While only one π-helix is shown, the 222 symmetry of the tetramer means that this steric clash would have to be overcome twice to form a stable tetramer [Fig. 5(B)]. A similar clash is predicted for the ΔY118 variant based on the structure determined here: a shift in residues 111–114 due to disruption of the helix is seen in the deletion mutant that would prevent tetramerization [Fig. 5(C)]. However, solution studies indicate that the primary ΔY118 SsuE oligomer is the tetramer.[24] Therefore, the less rigid broken helix must allow rearrangement of residues 115–119 to allow for packing of residues 111–114 to regenerate the tetramerizaton interface in solution.

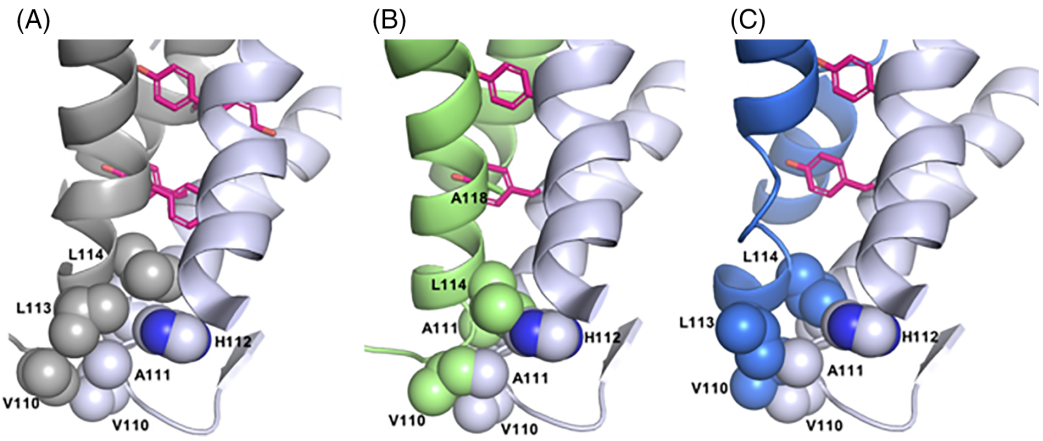

Figure 5. Disruption of the tetrameric interface in Y118A and Δ118 SsuE. (A) The tetramerization interface of the wild-type SsuE structure with monomers shown in grey and lavender. The Y118 residue is shown in in pink, and the residues that comprise one tetramerization interface are shown in space-filling representation. Note that for the wild-type SsuE structure, the interface forms a complementary hydrophobic surface between two monomers. (B) Y118A SsuE (green) docked with a wild-type dimer to form a tetramer (lavender). The space-filling model shows that the continuous α-helix of the variant changes the N-terminal pack compared to the π-helix, causing steric clash (atoms occupying the same three dimensional space). (C) ΔY118 SsuE variant (blue) docked with a wild-type dimer (lavender). The Y118 deletion disrupts the π-helix, making a nonhelical center section, which displaces the N-terminus causing an even greater steric clash that prevents tetramerization.

Kinetic properties of the SsuE and MsuE π-helix chimeras

The insertional residue that generates the π-helix in SsuE is Y118, whereas in MsuE this residue is H126. Aromatic π-stacking may be key in the tetramerization interaction mediated by these residues. We therefore hypothesized that interchanging these residues would result in chimeric proteins (Y118H SsuE and H126Y MsuE) that had kinetic values unchanged in comparison to the wild-type enzymes. Initial kinetic studies were performed to evaluate the reductase activity of wild-type *P. aeruginosa* MsuE, as kinetic parameters had not been determined previously. The purified MsuE did not possess a characteristic flavin spectrum similar to SsuE. The wild-type MsuE enzyme had a higher k_{cat}/K_m value $(32 \pm 10) \times 10^4$ M^{-1} s^{-1} for NADH compared to $(1.9 \pm 0.4) \times 10^4$ M^{-1} s^{-1} for NADPH (Table I). A kinetic preference for NADH was previously observed with MsuE from *P. fluorescens*.[15] Similar k_{cat}/K_m values were obtained for FMN varying NADH or NADPH at $(7 \pm 1) \times 10^6$ M^{-1} s^{-1} and $(6 \pm 2) \times 10^6$ M^{-1} s^{-1}, respectively. The H126Y MsuE variant showed similar kinetic parameters as wild-type for both NADH and NADPH (Table I). The comparable kinetic parameters suggest that substitution of the His insertional residue with Tyr did not disrupt the ability of the enzyme to reduce FMN. Unexpectedly, the Y118H SsuE variant behaves like the Y118A SsuE and ΔY118 SsuE variants. Y118H SsuE showed no measurable activity under any of the assay conditions tested, suggesting that Y118H SsuE protects the reduced FMN from release and reoxidation, preventing the enzyme from entering the steady state.

Coupled assays that include the FMN reductase (SsuE or MsuE) and monooxygenase (SsuD or MsuD) were performed to evaluate the ability of the SsuE and MsuE variants to effectively transfer flavin to their respective monooxygenase partner. Desulfonation activity by the monooxygenase was observed with the H126Y MsuE/MsuD pair with a k_{cat}/K_m value of $(4 \pm 2) \times 10^4$ M^{-1} s^{-1}, comparable to the wild-type MsuE/MsuD value of $(3 \pm 1) \times 10^4$ M^{-1} s^{-1}(Table II). Although activity was observed, the fit to the initial rates obtained in the assay were not optimal, and suggested the H126Y MsuE variant was not effectively coupled with MsuD (Supporting Information Fig. S1). As it is possible that the reduced flavin may be released from the Y118H SsuE when triggered by interaction with SsuD, desulfonation was also measured with this variant despite the enzyme's inability to enter the steady state for reductase activity. However, there was no measurable desulfonation activity observed in coupled assays monitoring sulfite production with the Y118H SsuE variant and SsuD, compared to the wild-type SsuE/SsuD value of $(3.1 \pm 0.3) \times 10^4$ M^{-1} s^{-1} (Table II).

The release of $FMNH_2$ from the reductase enzymes may be triggered by monooxygenase binding, and the π-helix insertional residue may be important in this interaction. Therefore, the MsuE and SsuE variants were evaluated to see if they could transfer reduced flavin to the opposite monooxygenase partner. The kinetic parameters for desulfonation by SsuD were similar with wild-type MsuE as when SsuE was included in the assay with a k_{cat}/K_m value of $(7 \pm 2) \times 10^4$ M^{-1} s^{-1} (Table II). Similarly, SsuE was able to effectively transfer flavin to MsuD with a k_{cat}/K_m value of $(1.9 \pm 0.7) \times 10^4$ M^{-1} s^{-1}. These kinetic parameters were analogous to the k_{cat}/K_m value of $(3.1 \pm 0.3) \times 10^4$ M^{-1} s^{-1} obtained in the SsuE /SsuD coupled reaction. Comparable desulfonation activity was observed with the H126Y MsuE variant regardless of which monooxygenase was included in the assay (Table II). However, the Y118H SsuE variant was unable to support flavin transfer to either monooxygenase. The absence of desulfonation activity with the Y118H SsuE variant suggests that the substitution of histidine for tyrosine did not maintain the same functional properties to support catalysis as observed for H126Y MsuE.

Discussion

The π-helix, which was originally thought to be a rare occurrence, is now considered a more prevalent secondary structure in enzymes. It has been proposed that some π-helices are generated by the insertion of an amino acid within a conserved α-helix found in other members within a family.[21,22] The overall conformation of the conserved helix in the protein family would need to be adjusted to accommodate the insertional residue.[22] Furthermore, the instability of the π-helix would destabilize the structure of a protein

Table I. *Steady-State Kinetic Parameters for Wild-Type and Variants of MsuE and SsuE Measuring NAD(P)H-Dependent FMN Reductase Activity*

	NADH			NADPH		
	k_{cat} (s^{-1})	K_{NADH} (M, $\times 10^{-6}$)	k_{cat}/K_{NADH} (M^{-1} s^{-1}, $\times 10^4$)	k_{cat} (s^{-1})	K_{NADPH} (M, $\times 10^{-6}$)	k_{cat}/K_{NADPH} (M^{-1} s^{-1}, $\times 10^4$)
Wild-type MsuE	19 ± 3	60 ± 20	32 ± 10	1.3 ± 0.1	70 ± 10	1.9 ± 0.4
H126Y MsuE	15 ± 3	100 ± 50	14 ± 7	0.75 ± 0.05	60 ± 10	1.2 ± 0.3
Wild-type SsuE	3.0 ± 0.1	57 ± 5	5.2 ± 0.5	3.7 ± 0.4	80 ± 20	5 ± 2
Y118H SsuE*	—	—	—	—	—	—

* Values could not be determined within the experimental conditions.

Table II. *Desulfonation Activity with the Wild-Type and Variants of SsuE and MsuE*

	k_{cat} (s^{-1})	K_m (M, $\times 10^{-6}$)	k_{cat}/K_m (M^{-1} s^{-1}, $\times 10^4$)
Wild-type MsuE/MsuD*	0.38 ± 0.03	15 ± 6	2.5 ± 1.0
Wild-type MsuE/SsuD†	1.4 ± 0.1	19 ± 4	7 ± 2
H126Y MsuE/MsuD	0.29 ± 0.03	8 ± 5	4 ± 2
H126Y MsuE/SsuD	0.96 ± 0.04	24 ± 5	4.0 ± 0.9
Wild-type SsuE/SsuD	1.2 ± 0.1	39 ± 5	3.1 ± 0.3
Wild-type SsuE/MsuD	0.42 ± 0.04	22 ± 8	1.9 ± 0.7
Y118H SsuE/SsuD‡	—	—	—
Y118H SsuE/MsuD	—	—	—

* Assays to determine desulfonation with activity with MsuD measured oxidation of methanesulfonate as described in Materials and Methods.

† Assays to determine desulfonation activity with SsuD measured oxidation of octanesulfonate as described in Materials and Methods.

‡ Values could not be determined within the experimental conditions.

relative to members of the protein family that retain an α-helix. Therefore, the generation of a π-helix would be selected against if it did not provide a gain-of-function for the enzyme.

The π-helix identified in the FMN-dependent reductase SsuE is hypothesized to be generated by the insertion of a Tyr in the conserved α4-helix.[16] The conserved nature of the π-helix in the two-component NAD(P)H:FMN reductases MsuE and SfnF (albeit by insertion of a histidine at the same site) suggests that it plays a defined mechanistic role for this subgroup of enzymes that diverges from FMN-bound reductases within this family, such as ArsH and YdhA. The π-helix in SsuE located at the tetramer interface has been proposed to trigger the oligomeric changes necessary for protein–protein interactions with SsuD. Alternatively, introduction of the π-helix may result in a more flexible protein capable of release of the reduced FMN to the monooxygenase partner.[16]

Previous studies have shown that the Y118A SsuE, which removes the side chain potentially involved in aromatic π-stacking across the tetramer interface, is incapable of release of the reduced flavin and is predominantly dimeric in solution. In agreement with these data, helix 4 of the Y118A SsuE structure is a continuous α-helix, like those of reductases that do not release their flavin. Perplexingly, the ΔY118 SsuE protein, which deletes the entire insertional residue, is incapable of releasing the reduced flavin but is tetrameric in solution. The structure determined here shows that helix 4 of ΔY118 SsuE is broken and the protein is dimeric in the crystal. The more flexible nature of the broken ΔY118 SsuE helix 4 may allow it to repack as a tetramer. In other words, removal of the sidechain reverts helix 4 to and α-helix as seen in the homologous single component reductases, whereas removal of the insertional residue altogether generates a unique conformation—neither α- nor π-helix.

The insertional residue in SfnF and MsuE is a histidine and is positioned at the bulge site of the π-helix in the three-dimensional structure of SfnF. This position is homologous to Y118 in SsuE, also at the bulge of the π-helix. A histidine insertional residue would still be able to form similar interactions as Tyr118 in SsuE. While MsuE is from *P. aeruginosa* and SsuE is from *E. coli*, they have a high amino acid sequence identity in the π-helical region. Therefore, interchanging the proposed insertional residues, one would expect comparable kinetics effects: Y118H SsuE and H126Y MsuE should be kinetically equivalent. Instead, Y118H SsuE is kinetically equivalent to Y118A and ΔY118 SsuE, whereas H126Y MsuE is equivalent to wild-type MsuE. Indeed, H126Y MsuE can donate $FMNH_2$ to MsuD and SsuD with comparable success, and within error to wild-type MsuE. The results suggest that a protein–protein docking interaction for flavin transfer is not severely impacted by the generation of the variant. The less than optimal fit for the kinetic parameters could be due to a slight alteration of the protein–protein interaction region during flavin transfer. Furthermore, the Y118H SsuE is incapable of releasing $FMNH_2$ in the reductase assay, and is not triggered to release the flavin by addition of SsuD or MsuD in the desulfonation assay.

A structure-based sequence alignment for the NADPH:FMN reductases and variants discussed herein shows that the "insertional residue" hypothesis is problematic (Fig. 6). First, when considering the rmsd of α-carbons, the Y118 residue of SsuE and the H126 residue of SfnF do not result in a gap (insertion) within helix 4. Furthermore, ChrR, a quinone reductase from *E. coli*, is an FMN reductase with a flavodoxin fold and an α-helical helix 4 that is more structurally distant than the other homologs discussed so far (2.8 Å rmsd for 164 Cα).[26] Nevertheless, ChrR has a tyrosine at the equivalent Y118-SsuE site that aligns directly with that of the alanine in the Y118A SsuE variant. Clearly, a tyrosine at the insertion site in ChrR is not sufficient to develop a π-helix and convert a reductase into one that can deliver reduced FMN to a monooxygenase in a two-component system. Two possibilities may explain the alternative functions in the two-component FMN

reductases. First, the presence of the π-helix may not fully explain the ability of two component reductases to release flavin to a monooxygenase and other structural features may also be important. For example, the C-terminal ~20 residues have never been resolved in these reductases. A reductase–monooxygenase complex structure would be of significant import in deciding this question. Second, if the π-helix is indeed of functional significance, generation of a π-helix through evolutionary adaptation is not as simple as insertion of a residue, and compensatory variations are likely also required for gain-of-function.

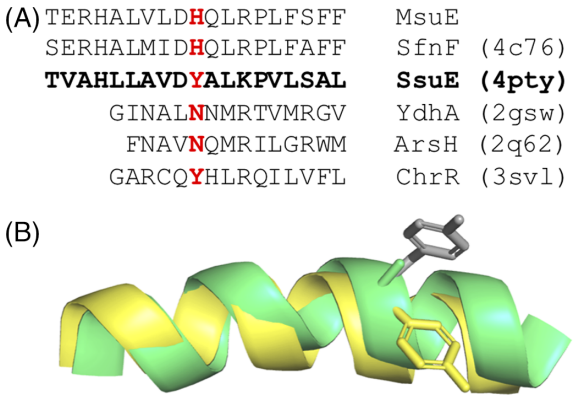

Figure 6. Structure-based alignment generated by PDBeFOLD. (A) The helix 4 sequence is shown for each protein, with PDB codes shown in parenthesis, if structure determined: *P. aeruginosa* MsuE (used for kinetics work herein), presumed to be a π-helix; *P. putida* SfnF, π-helix; *E. coli* SsuE, π-helix; *B. subtilis* YhdA, α-helix; *S. meliloti* ArsH, α-helix; *E. coli* ChrR, α-helix. The insertional residue at the bulge in the π-helix or the residue at the homologous site in the α-helix is shown in red. (B) Overlay of wild-type SsuE π-helix (gray), with Y118A SsuE (green) and ChrR (yellow) α-helices. The grey helix is not shown for simplicity because the bulge obscures the other structures. Note that the tyrosine of ChrR is in the structurally equivalent position to Y118 of SsuE; however, ChrR has an α-helix like Y118A SsuE and not a π-helix like wild-type. The orientation of the tyrosine in ChrR prevents this residue from participating in tetramerization at the interface.

Materials and Methods

Materials

The *P. aeruginosa* (PAO1) cell line was purchased from ATCC type culture collection (ATCC15692). *E. coli* strains [XL-1 Blue and BL21(DE3)] were purchased from Stratagene (La Jolla, CA). Plasmid vectors and pET21a were obtained from Novagen (Madison, WI). DNA primers were synthesized by Invitrogen (Carlsbad, CA). Pfu Turbo DNA polymerase was purchased from Agilent (La Jolla, CA). Zero Blunt PCR Cloning Kit was from ThermoFisher (Waltham, MA). Difco-brand Luria-Bertani (LB) media was purchased from Becton, Dickinson and company (Sparks, MD). Phenyl Sepharose™ 6 Fast Flow (high sub) was purchased from GE Healthcare Biosciences, (Uppsala, Sweden). Macro-Prep® High Q Support (Bio-Rad Laboratories, Hercules, CA). sodium dodecyl sulfate (SDS) and acrylamide were purchased from Biorad (Hercules, CA). Buffer components and chemicals for kinetic assays were purchased from Sigma (St. Louis, MO). Isopropyl-β-D-1-thiogalactoside (IPTG), sodium chloride, and glycerol were obtained from Macron Fine Chemicals (Center Valley, PA). Oligonucleotide primers were purchased from Invitrogen (Carlsbad, CA).

Cloning and site-directed mutagenesis of MsuE and SsuE

Cloning of the *msuE* and *msuD* gene into an expression vector was performed by PCR amplification of the gene from *P. aeruginosa*. A 100 mL culture of *P. aeruginosa* was grown overnight at 37°C. The cells were pelleted following an overnight incubation, and the chromosomal DNA from *P. aeruginosa* was extracted using the QIAprep Spin Miniprep Kit. The *msuE* gene was PCR-amplified using the primers (5′-GAT GAT CAT ATG ACC AGC CCC TTC AAA) and (5′-GAT GAT CTC GAG TCA GGC GAT CTT CAA) which included engineered *Nde* I and *Xho* I restriction sites for ligation into the pET21a expression vector. A hairpin existed between the *msuC* and *msuD* operon, which made in difficult to amplify *msuD* from the genome. Both msuC and msuD were first PRC-amplified using the primers (5′-ATGAACGTGTTCTGGTTCCTCCC) and (5′-TATGGG-TAGCTCGAGTCATGAGTAG), and the resulting PCR product was cloned in to the pCR-Blunt cloning vector using the Zero Blunt PCR Cloning Kit. The DNA vectors containing representative clones were submitted for DNA sequence analysis (Eurofins/Genomics, Louisville, KY). The *ssuD* gene was PCR-amplified from the pCR-Blunt vector containing *msuC/msuD* using the primers (5′-GCGCATATGAACGTGTTCTGGTTC) and (5’ CCCC TCGAGTCAAGCGCC), which included engineered *Nde* I and *Xho* I restriction sites for ligation into the pET21a expression vector. The T7 RNA polymerase-dependent expression vector pET21a (Novagen, Madison, WI) and the *msuE* and *msuD* PCR products were digested with restriction enzymes *Nde* I and *Xho* I for 1 h at 37°C. A 3:1 ratio of either *msuE* or *msuD* insert to pET21 a vector were ligated with T4 DNA ligase at 16°C overnight, and transformed into Top10 cells following the overnight incubation. The DNA vectors containing representative clones were submitted for DNA sequence analysis (Eurofins/Genomics, Louisville, KY).

Variants of Tyr118 in SsuE and His 126 in MsuE were generated to investigate the importance of these residues in preserving the π-helix. The primers were designed as 27-base oligonucleotides for the Y118H SsuE and H126Y MsuE variants. The primers were ordered from Life Technologies by substituting the *ssuE* codon TAT representing Tyr118 with TCT, and substituting the *msuE* codon TCT representing His with TAT. The Qiagen kit plasmid purification protocol

was utilized to prepare the SsuE plasmid for site-directed mutagenesis. Following site-directed mutagenesis, the SsuE variants were confirmed through DNA sequencing analysis (Eurofins/Genomics, Louisville, KY). The FMN-dependent reductase and monooxygenase enzymes were expressed and purified in *E. coli* strain BL21(DE3) as previously described.[2] The concentrations of SsuD and SsuE proteins were determined from A_{280} measurements using a molar extinction coefficient of 47.9 and 20.3 mM^{-1} cm^{-1}, respectively.[2] Concentrations of MsuD and MsuE were determined from A_{280} measurements using a molar extinction coefficient of 49.4 and 7.5 mM^{-1} cm^{-1}, respectively.

Steady-state kinetic assays of SsuE and MsuE

The NAD(P)H oxidase activity for wild-type MsuE was initially evaluated to determine steady-state kinetic parameters and substrate specificity for MsuE. Kinetic parameters for FMN were determined with 0.1 μM wild-type or H126Y MsuE at varying concentrations of FMN (0.01–3 μM) with fixed concentrations of NADPH (100 μM), or varying concentrations of FMN (0.3–13 μM) with fixed concentrations of NADH (200 μM). The kinetic parameters for NADH and NADPH were determined with 0.1 μM MsuE at varying concentrations of NADPH (2.5–150 μM) with fixed concentrations of FMN (2 μM), or varying concentrations of NADH (2.5–150 μM) with fixed concentrations of FMN (10 μM). The SsuE enzyme can utilize either NADH or NADPH in NAD(P)H oxidase assays, but has a flavin preference for FMN. Steady-state kinetic parameters for wild-type or Y118H SsuE were performed as previously described to maintain consistency with previous studies.[2] All assays were performed in triplicate, and the initial rates were obtained by monitoring the decrease in absorbance at 340 nm with the oxidation of the reduced pyridine nucleotide. The steady-state kinetic parameters were determined by fitting the data to the Michaelis–Menten equation.

The steady-state coupled assay was performed as previously described.[4] The reactions were initiated with the addition of 500 μM NADPH into a reaction mixture containing wild-type or Y118H SsuE (0.6 μM), FMN (2 μM), SsuD (0.2 μM), and varied concentrations of octanesulfonate (10–1000 μM) in 25 mM Tris–HCl (pH 7.5), and 0.1 M NaCl at 25°C. The desulfonation assays with SsuD were also performed using wild-type and Y118H MsuE (0.6 μM) in the reaction to provide reduced flavin The reaction was quenched after 3 min with 8 M urea, and the sulfite product was quantified as previously described.[4] Conditions for the coupled reactions with MsuD were performed similar to SsuD, but the concentration of methanesulfonate was varied from 5–500 μM. All assays were performed in triplicate, and steady-state kinetic parameters were determined by fitting the data to the Michaelis–Menten equation.

Crystallization of the SsuE variants

All crystals were grown in hanging drops composed of 1.5 μL of well solution and 1.5 μL of protein in 10 mM HEPES pH 8.5, 100 mM NaCl, and 10% (v/v) glycerol. The apo Y118A SsuE crystals were grown using 68 mg/mL protein and a well solution of 100 mM Tris HCl pH 8.5 and 800 mM lithium sulfate. Crystals grew within 5 days and were cryoprotected with well solution containing 2.25 M lithium sulfate prior to flash cooling. The FMN-bound Y118A SsuE crystals were grown using 12.5 mg/mL protein, supplemented with flavin mononucleotide (FMN) to 10 mM, before combining with well solution composed of 200 mM sodium thiocyanate pH 6.9 and 20% (w/v) PEG 3350. Crystals grew within 5 days and were cryoprotected with well solution containing 30% glycerol prior to flash cooling. The Δ118 SsuE crystals were grown using 35 mg/mL protein and a well solution composed of 100 mM CHES: NaOH pH 9.5 and 30% (w/v) PEG 3000. Crystals grew within 5 days and were cryoprotected with well solution containing 25% glycerol prior to flash cooling.

Data collection and structural determination of the SsuE variants

Diffraction data were collected remotely using BluIce on beamline 12–2 at the Stanford Synchrotron Radiation Lightsource (SSRL, Menlo Park, CA).[27] All data sets were collected at a wavelength of 0.97946 Å with 0.15° oscillation and 0.2 s exposure at a temperature of 100 K. For Y118A SsuE, 180° of data were collected at a detector distance of 325 mm and processed to 1.95 Å in XDS.[28] A phasing solution was determined by molecular replacement in Phaser[3] using apo SsuE (PDB: 4PTY) as a model with a resulting LLG of 1462 and TFZ of 39.9. For FMN-bound Y118A SsuE, 360° of data were collected at a detector distance of 315 mm and processed to 1.71 Å using AutoPROC.[29] A phasing solution was determined by molecular replacement, as above, with a resulting LLG of 904 and TFZ of 31.8. For Δ118 SsuE, 240° of data were collected at a detector distance of 250 mm and processed to 1.55 Å using AutoPROC[2]. A phasing solution was determined by molecular replacement as above with a resulting LLG of 2,581 and TFZ of 47.9. For each structure, rounds of model building and refinement were completed in Coot and Phenix Refine and waters were placed by Phenix Refine, corrected manually and verified, using a $2mF_oDF_c$ electron density map contoured at 1.5 σ, following a round of refinement.[30,31] For FMN-bound Y118A SsuE, complete density for the active site FMN was visible following molecular replacement, but was not modeled until after refining the polypeptide backbone. For the Δ118 SsuE variant, TLS refinement was used during the last two rounds of refinement. Statistics for data collection and refinement are listed in Table III.

Table III. *Data Collection and Refinement Statistics*

	apo Y118A SsuE	Y118A SsuE(+FMN)	apo Δ118 SsuE
Data collection			
Spacegroup	$P2_12_12_1$	$C222_1$	$P2_12_12_1$
Unit cell (Å)	a = 39.5, b = 41.5, c = 189	a = 80.9, b = 110.8, c = 41.7	a = 40.9, b = 41.8, c = 182.3
Resolution range (Å)	38.0–1.95	33.34–1.71	30.8–1.55
Completeness (%)	97.7 (99.2)	99.6 (99.7)	99.9 (99.9)
Total reflections	174,752	272,611	397,291
Unique reflections	23,620	20,849	46,854
I/σ	17.9 (7.0)	24.9 (2.1)	19.3 (3.0)
R_{merge}*	7.8 (31.0)	5.7 (>100)	9.3 (91.0)
R_{pim}†	4.7 (18.3)	1.6 (32.7)	3.3 (33.7)
Multiplicity	7.4 (7.6)	13.1 (13.3)	8.5 (8.1)
Refinement			
Resolution range (Å)	39.5–1.95	33.34–1.71	30.8–1.55
No. of reflections	23,063	20,841	46,844
R_{work}/R_{free}‡	18.5/23.7	18.4/20.7	16.0/17.8
No. of nonhydrogen atoms	2863	1500	2927
Protein	2734	1356	2720
Ligand/ion	5	87	12
Water	124	57	195
Ramachandran favored (%)	100	98.3	100
Ramachandran outliers (%)	0	0	0
Wilson B	19.8	25.9	15.3
Average B (Å^2)	24.7	28.4	20.8
Protein	24.7	28.3	20.4
Ligand/ion	33.1	26.0	21.9
R.m.s. deviations			
Bond lengths (Å)	0.012	0.011	0.009
Bond angles (°)	1.1	1.27	1.03

Data were collected on beamline 12–2 at the Stanford Synchrotron Radiation Lightsource. Values in parentheses are for the highest resolution shell.

* $R_{merge} = \sum_{hkl}|I_{hkl} - \langle I\rangle_{hkl}|/\sum_{hkl}I_{hkl}$, where $I_{hkl}$is the intensity of reflection hkl and $\langle I\rangle$ is the mean intensity of related reflections.

† $R_{pim} = \sum_{hkl}\sqrt{1/n-1}|I_{hkl}-\langle I\rangle_{hkl}|/\sum_{hkl}I_{hkl}$, where n is the multiplicity of related reflections.

‡ $R = \sum||F_o| - |F_c||/\sum|F_o|$, where F_o = to the observed structure factors and F_c = structure factors calculated from the model. A total of 5% of the reflections were initially reserved to create an R_{free} test set used during each subsequent round of refinement.

Crystallographic model analysis

The apo Y118A, FMN-bound Y118A, and Δ118 SsuE models were analyzed by MolProbity and each showed good geometry with no Ramachandran outliers.[32] Apo Y118A SsuE has two monomers in the asymmetric unit with density for residues 1–172 and 1–174. Residues H148 and R149 are in a surface loop with discontinuous backbone density in both chains. The apo Y118A SsuE model contains 124 water molecules and one sulfate ion bound in the phosphate binding site of FMN (lithium sulfate was the precipitant and cryoprotectant). The Y118A SsuE variant with FMN bound has one monomer in the asymmetric unit with continuous density for residues 1–172, as well as 59 waters and 1 glycerol. Complete density for the active site FMN is present [Supporting Information Fig. S2(B)]. A second FMN with partial electron density for two conformations is stacked along the isoalloxazine ring of the active site FMN. The mF_o–DF_c map shows positive density over the positions of the isoalloxazine ring oxygens in both conformers. It is possible that water molecules maintain partial occupancy in these positions. The Δ118 SsuE variant has two monomers in the asymmetric unit with continuous density for residues 1–172 and 1–173, with 193 waters and 2 glycerol molecules. The two monomers seen in the asymmetric unit of apo Y118A and Δ118 SsuE form a dimeric assembly. The FMN-bound Y118A SsuE variant also crystallized in this dimeric assembly, but it is generated using symmetry operations with the monomer in the adjacent asymmetric unit. PISA predicts interface surface areas of 1125, 1196, and 1171 Å^2 for the three structures, consistent with the previously reported wild-type dimer interface of 1160 Å^2.[16,33]

Acknowledgments

Research reported in this publication was made possible by funds from The National Science Foundation (MCB-1244320 to HRE and CHE-1403293 to ALL). JSM was supported by the National Institutes of Health Graduate Training Program in the Dynamic Aspects of Chemical Biology (T32 GM008545) and by an American Heart Association Predoctoral Fellowship (18PRE33960374). Use of the Stanford Synchrotron Radiation Lightsource, SLAC National

Accelerator Laboratory, is supported by the U.S. Department of Energy, Office of Science, Office of Basic Energy Sciences under Contract No. DE-AC02-76SF00515. The SSRL Structural Molecular Biology Program is supported by the Department of Energy Office of Biological and Environmental Research, and by the NIH and NIGMS (including P41GM103393). The authors thank the staff at the SSRL for their generous assistance. They are grateful to KM Meneely for technical assistance.

References

1. Eichhorn E, van der Ploeg JR, Leisinger T (1999) Characterization of a two-component alkanesulfonate monooxygenase from *Escherichia coli*. J Biol Chem 274: 26639–26646.
2. Gao B, Ellis HR (2005) Altered mechanism of the alkanesulfonate FMN reductase with the monooxygenase enzyme. Biochem Biophys Res Commun 331:1137–1145.
3. Gao B, Ellis HR (2007) Mechanism of flavin reduction in the alkanesulfonate monooxygenase system. Biochim Biophys Acta 1774:359–367.
4. Zhan X, Carpenter RA, Ellis HR (2008) Catalytic importance of the substrate binding order for the FMNH2-dependent alkanesulfonate monooxygenase enzyme. Biochemistry 47:2221–2230.
5. Robbins JM, Ellis HR (2012) Identification of critical steps governing the two-component alkanesulfonate monooxygenase catalytic mechanism. Biochemistry 51: 6378–6387.
6. Robbins JM, Ellis HR (2014) Steady-state kinetic isotope effects support a complex role of Arg226 in the proposed desulfonation mechanism of alkanesulfonate monooxygenase. Biochemistry 53:161–168.
7. van der Ploeg JR, Cummings NJ, Leisinger T, Connerton IF (1998) *Bacillus subtilis* genes for the utilization of sulfur from aliphatic sulfonates. Microbiology 144:2555–2561.
8. Hummerjohann J, Kuttel E, Quadroni M, Ragaller J, Leisinger T, Kertesz MA (1998) Regulation of the sulfate starvation response in *Pseudomonas aeruginosa*: role of cysteine biosynthetic intermediates. Microbiology 144: 1375–1386.
9. Bentley R, Chasteen TG (2004) Environmental VOSCs—formation and degradation of dimethyl sulfide, methanethiol and related materials. Chemosphere 55: 291–317.
10. Endoh T, Habe H, Yoshida T, Nojiri H, Omori T (2003) A CysB-regulated and sigma54-dependent regulator, SfnR, is essential for dimethyl sulfone metabolism of *Pseudomonas putida* strain DS1. Microbiology 149: 991–1000.
11. Endoh T, Kasuga K, Horinouchi M, Yoshida T, Habe H, Nojiri H, Omori T (2003) Characterization and identification of genes essential for dimethyl sulfide utilization in *Pseudomonas putida* strain DS1. Appl Microbiol Biotechnol 62:83–91.
12. Endoh T, Habe H, Nojiri H, Yamane H, Omori T (2005) The sigma54-dependent transcriptional activator SfnR regulates the expression of the *Pseudomonas putida* sfnFG operon responsible for dimethyl sulphone utilization. Mol Microbiol 55:897–911.
13. Habe H, Kouzuma A, Endoh T, Omori T, Yamane H, Nojiri H (2007) Transcriptional regulation of the sulfate-starvation-induced gene sfnA by a sigma54-dependent activator of *Pseudomonas putida*. Microbiology 153:3091–3098.
14. Kouzuma A, Endoh T, Omori T, Nojiri H, Yamane H, Habe H (2008) Transcription factors CysB and SfnR constitute the hierarchical regulatory system for the sulfate starvation response in *Pseudomonas putida*. J Bacteriol 190:4521–4531.
15. Wicht DK (2016) The reduced flavin-dependent monooxygenase SfnG converts dimethylsulfone to methanesulfinate. Arch Biochem Biophys 604:159–166.
16. Driggers CM, Dayal PV, Ellis HR, Karplus PA (2014) Crystal structure of *Escherichia coli* SsuE: defining a general catalytic cycle for FMN reductases of the flavodoxin-like superfamily. Biochemistry 53:3509–3519.
17. Binter A, Staunig N, Jelesarov I, Lohner K, Palfey BA, Deller S, Gruber K, Macheroux P (2009) A single intersubunit salt bridge affects oligomerization and catalytic activity in a bacterial quinone reductase. FEBS J 276: 5263–5274.
18. Vorontsov II, Minasov G, Brunzelle JS, Shuvalova L, Kiryukhina O, Collart FR, Anderson WF (2007) Crystal structure of an apo form of *Shigella flexneri* ArsH protein with an NADPH-dependent FMN reductase activity. Protein Sci 16:2483–2490.
19. Deller S, Sollner S, Trenker-El-Toukhy R, Jelesarov I, Gübitz GM, Macheroux P (2006) Characterization of a thermostable NADPH:FMN oxidoreductase from the mesophilic bacterium *Bacillus subtilis*. Biochemistry 45: 7083–7091.
20. Deller S, Macheroux P, Sollner S (2008) Flavin-dependent quinone reductases. Cell Mol Life Sci 65:141–160.
21. Weaver TM (2000) The pi-helix translates structure into function. Protein Sci 9:201–206.
22. Cooley RB, Arp DJ, Karplus PA (2010) Evolutionary origin of a secondary structure: π-helices as cryptic but widespread insertional variations of α-helices that enhance protein functionality. J Mol Biol 404: 232–246.
23. Musila JM, Ellis HR (2016) Transformation of a flavin-free FMN reductase to a canonical flavoprotein through modification of the π-helix. Biochemistry 55: 6389–6394.
24. Musila J, Forbes D, Ellis HR (2018) Functional evaluation of the π-helix in the NAD(P)H:FMN reductase of the alkanesulfonate monooxygenase system. Biochemistry 57:4469–4477.
25. Dayal PV, Singh H, Busenlehner LS, Ellis HR (2015) Exposing the alkanesulfonate monooxygenase protein-protein interaction sites. Biochemistry 54: 7531–7538.
26. Eswaramoorthy S, Poulain S, Hienerwadel R, Bremond N, Sylvester MD, Zhang YB, Berthomieu C, Van Der Lelie D, Matin A (2012) Crystal structure of ChrR—a quinone reductase with the capacity to reduce chromate. PLoS One 7:e36017.
27. McPhillips TM, McPhillips SE, Chiu HJ, Cohen AE, Deacon AM, Ellis PJ, Garman E, Gonzalez A, Sauter NK, Phizackerley RP, Soltis SM, Kuhn P (2002) Blu-ice and the distributed control system: software for data acquisition and instrument control at macromolecular crystallography beamlines. J Synchrotron Radiat 9: 401–406.
28. Kabsch W (2010) XDS. Acta Cryst D66:125–132.
29. Vonrhein C, Flensburg C, Keller P, Sharff A, Smart O, Paciorek W, Womack T, Bricogne G (2011) Data processing and analysis with the autoPROC toolbox. Acta Cryst D67:293–302.

30. Emsley P, Cowtan K (2004) Coot: model-building tools for molecular graphics. Acta Cryst D60:2126–2132.
31. Adams PD, Grosse-Kunstleve RW, Hung LW, Ioerger TR, McCoy AJ, Moriarty NW, Read RJ, Sacchettini JC, Sauter NK, Terwilliger TC (2002) PHENIX: building new software for automated crystallographic structure determination. Acta Cryst D58: 1948–1954.
32. Chen VB, Arendall WB III, Headd JJ, Keedy DA, Immormino RM, Kapral GJ, Murray LW, Richardson JS, Richardson DS (2010) MolProbity: all-atom structure validation for macromolecular crystallography. Acta Cryst D66:12–21.
33. Krissinel E, Henrick K (2004) Secondary-structure matching (SSM), a new tool for fast protein structure alignment in three dimensions. Acta Cryst D60:2256–2268.